

PredRNN++: Towards A Resolution of the Deep-in-Time Dilemma in Spatiotemporal Predictive Learning

Yunbo Wang¹ Zhifeng Gao¹ Mingsheng Long¹ Jianmin Wang¹ Philip S. Yu¹

Abstract

We present *PredRNN++*, an improved recurrent network for video predictive learning. In pursuit of a greater spatiotemporal modeling capability, our approach increases the transition depth between adjacent states by leveraging a novel recurrent unit, which is named *Causal LSTM* for re-organizing the spatial and temporal memories in a cascaded mechanism. However, there is still a dilemma in video predictive learning: increasingly deep-in-time models have been designed for capturing complex variations, while introducing more difficulties in the gradient back-propagation. To alleviate this undesirable effect, we propose a *Gradient Highway* architecture, which provides alternative shorter routes for gradient flows from outputs back to long-range inputs. This architecture works seamlessly with causal LSTMs, enabling *PredRNN++* to capture short-term and long-term dependencies adaptively. We assess our model on both synthetic and real video datasets, showing its ability to ease the vanishing gradient problem and yield state-of-the-art prediction results even in a difficult objects occlusion scenario.

1. Introduction

Spatiotemporal predictive learning is to make machines learn the physics by observing real events in videos. It is very intriguing and worth exploring that how to leverage this learning paradigm to benefit practical applications, such as precipitation forecasting (Shi et al., 2015; Wang et al., 2017), traffic flows prediction (Zhang et al., 2017) and physical interactions simulation (Lerer et al., 2016; Finn et al., 2016).

An accurate prediction of future frames depends on an effective modeling of the dynamical structures in previous contexts, where exist two situations: (1) Future predictions

significantly depend on nearby previous frames rather than distant prior inputs, which requires the learning system to foretell the object trajectories from recent events. (2) Moving objects are entangled in the contexts, it is hard to differentiate each of them and maintain their individual shapes in future predictions. This scenario requires the learning system to remember objects' original shapes in prior contexts before occlusion happens. To sum up, an effective predictive model should simultaneously and adaptively extract the short-term as well as long-term dependencies from videos.

1.1. Deep-in-Time Structures and Vanishing Gradients Dilemma in Spatiotemporal Modeling

Due to their ability to modeling sequential data, recurrent neural networks (RNNs) (Rumelhart et al., 1988; Werbos, 1990; Williams & Zipser, 1995) have been recently applied to video predictive learning (Ranzato et al., 2014). However, most contemporary works (Srivastava et al., 2015a; Shi et al., 2015; Patraucean et al., 2016) followed the traditional RNNs chain structure and did not fully utilize the network depth. The assignments between adjacent hidden states from one frame to the next are modeled by simple internal function mappings in RNN units, though theoretical evidence shows that deeper networks can be exponentially more efficient in both spatial feature extraction (Bianchini & Scarselli, 2014) and sequential information modeling (Pascanu et al., 2013).

Motivated by this, a well-performed video prediction model, *PredRNN* (Wang et al., 2017), applied complex nonlinear transition functions from one frame to the next, constructing a dual Long Short-Term Memory (LSTM) (Hochreiter & Schmidhuber, 1997) network with “deep-in-time” neural connections. Unfortunately, deep-in-time structures easily suffer from the vanishing gradient problem (Bengio et al., 1994; Pascanu et al., 2013), since the magnitude of the gradients may decay exponentially during back-propagation.

There is a dilemma in spatiotemporal modeling: the increasingly deep-in-time networks have been designed for complex video dynamics, while also introducing more difficulties in gradients propagation. Therefore, how to maintain a steady flow of derivatives in a deep-in-time predictive network, is a path worth exploring. Our key insight is to build adaptive connections among RNN states, providing

¹School of Software, Tsinghua University, Beijing, China. E-mail: wangyb15@mails.tsinghua.edu.cn, psyu@uic.edu. Correspondence to: Mingsheng Long <mingsheng@tsinghua.edu.cn>.

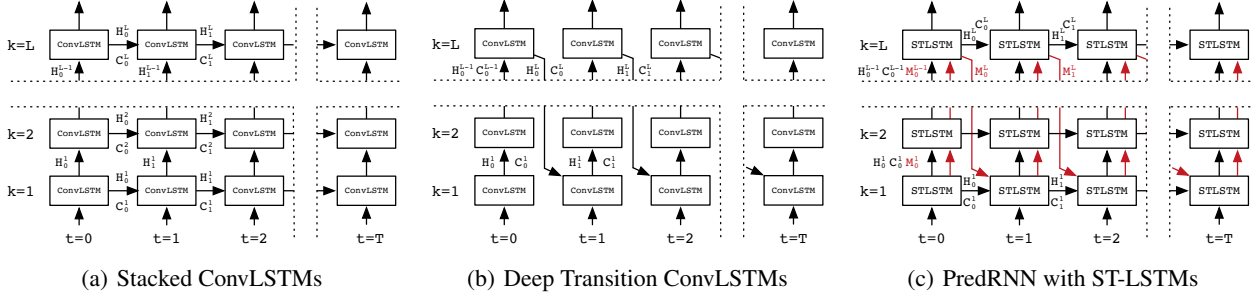


Figure 1. Comparison of data flows in (a) the stacked ConvLSTM network, (b) the deep transition ConvLSTM network, and (c) PredRNN with the spatiotemporal LSTM (ST-LSTM). The two memories of PredRNN work in parallel: the red lines in subplot (c) denote the deep transition paths of the spatial memory, while horizontal black arrows indicate the update directions of the temporal memories.

our model both longer paths and shorter paths at the same time, from input frames to the expected future predictions.

2. Related Work

Recurrent neural networks (RNNs) are widely used in video prediction. (Ranzato et al., 2014) constructed a RNN model to predict the next frames. (Srivastava et al., 2015a) adapted the sequence to sequence LSTM framework for video sequence prediction. (Shi et al., 2015) extended this model and present the convolutional LSTM (ConvLSTM) by plugging convolution operations in recurrent connections. (Wang et al., 2017) proposed a recurrent network with dual memory structures, in which the memory states are no longer constrained inside each LSTM unit, instead, they are allowed to zigzag across stacked RNN layers vertically and through all RNN states horizontally. (Finn et al., 2016) built a recurrent network to predict physical interactions using extra cues such as robot future actions. (Lotter et al., 2017) presented a variation of the ConvLSTM network, however, only working well for predicting the next one frame. Our model, by contrast, predicts a sequence into the future, which is obviously more challenging. (Villegas et al., 2017a) takes in image differences for short-term video dynamics. (Patraucean et al., 2016) predicts future images and optical flows. (Kalchbrenner et al., 2017) proposed a sophisticated model combining gated CNN and ConvLSTM structures. It estimates pixel values in a video one-by-one using the well-established but complicated PixelCNNs (van den Oord et al., 2016), thus severely suffers from low prediction efficiency.

Convolutional neural networks (CNNs) are also involved in video prediction, despite they only create representations for fixed size inputs. (Oh et al., 2015) defined a CNN-based autoencoder model for Atari games prediction. (De Brabandere et al., 2016) adapted filter operations of the convolutional network to the specific input samples. (Villegas et al., 2017b) proposed a three-stage framework with additional annotated human joints data to make longer predictions. To

deal with the inherent uncertainty of the future, (Mathieu et al., 2016; Vondrick et al., 2016; Bhattacharjee & Das, 2017) employed generative adversarial networks (Goodfellow et al., 2014; Denton et al., 2015) to preserve the sharpness of the generated frames. (Lu et al., 2017) combined this ideas with recurrent networks. Though we did not discuss adversarial networks in this paper, since we would like to focus on exploring new structures for spatiotemporal modeling, we believe integrating predictive models with adversarial training is quite an interesting research direction.

In summary, prior video prediction models yield different drawbacks. CNN-based approaches predict a limited number of frames in one pass. They focus on spatial appearances rather than the temporal coherence in long-term motions. The RNN-based approaches, in contrast, capture temporal dynamics with recurrent connections. However, their predictions suffer from the inherent weakness of RNNs: the famous vanishing gradient problem, thus particularly rely on closest frames. In our preliminary experiments, it was hard to preserve the shapes of the moving objects in generated future frames, especially after they overlapped. In this paper, we solve this problem by proposing a new gradient highway architecture, which absorbs knowledge from previous video frames and effectively leverages long-term information.

3. Revisiting Deep-in-Time Information Flows

A general method to increase the depth of RNNs is stacking multiple hidden layers. A typical stacked recurrent network for video prediction (Shi et al., 2015) can be presented as Figure 1(a). The recurrent unit, ConvLSTM, is designed to properly keep and forget past information via gated structures, and then fuse it with current spatial representations. Nevertheless, stacked ConvLSTMs do not add extra modeling capability to the step-to-step recurrent state transitions.

In our preliminary observations, increasing the step-to-step transition depth in ConvLSTMs can significantly improve its

modeling capability to the short-term dynamics. As shown in Figure 1(b), the hidden state, \mathcal{H} , and memory state, \mathcal{C} , are updated in a zigzag direction. The extended recurrence depth between horizontally adjacent states enables the network to learn complex non-linear transition functions of nearby frames in a short interval. However, it introduces vanishing gradient issues, making it difficult to capture long-term correlations from the video. Though a simplified cell structure, the recurrent highway (Zilly et al., 2017), might somewhat ease this problem, it sacrifices the spatiotemporal modeling power, exactly as the dilemma described earlier.

Based on the deep transition architecture, a well-performed predictive learning approach, PredRNN (Wang et al., 2017), added extra connections between adjacent time steps in a stacked spatiotemporal LSTM (ST-LSTM), in pursuit of both long-term coherence and short-term recurrence depth. Figure 1(c) illustrates its information flows. PredRNN leverages a dual memory mechanism and combines, by a simple concatenation with gates, the horizontally updated temporal memory \mathcal{C} with the vertically transferred spatial memory \mathcal{M} . Despite the favorable information flows provided by the spatiotemporal memory, this parallel memory structure followed by a concatenation operator, and a 1×1 convolution layer for a constant number of channels, is not an efficient mechanism for increasing the recurrence depth. Besides, as a straight-forward combination of the stacked recurrent network and the deep transition network, PredRNN still faces the same vanishing gradient problem as prior works.

4. PredRNN++

In this section, we would give detailed descriptions of the improved predictive recurrent neural network (PredRNN++). Compared with the above deep-in-time recurrent architectures, our approach has two key insights: First, it presents a new spatiotemporal memory mechanism, causal LSTM, in order to increase the recurrence depth from one time step to the next, and by this means, derives a more powerful modeling capability to fine-grained spatial correlations and short-term dynamics. Second, it attempts to solve gradient back-propagation issues for the sake of long-term video modeling. It constructs an alternative gradient highway, a shorter route from future outputs back to distant prior inputs.

4.1. Causal LSTM

Causal LSTM is enlightened by the idea of adding more non-linear layers to recurrent transitions, increasing the network depth from one state to the next. A schematic of this new recurrent unit is shown in Figure 2. A causal LSTM unit contains dual memories, the temporal memory, \mathcal{C}_t^k , and the spatial memory, \mathcal{M}_t^k , where the subscript t denotes the time step, while the superscript denotes the k^{th} hidden layer in a stacked causal LSTM network. The current temporal

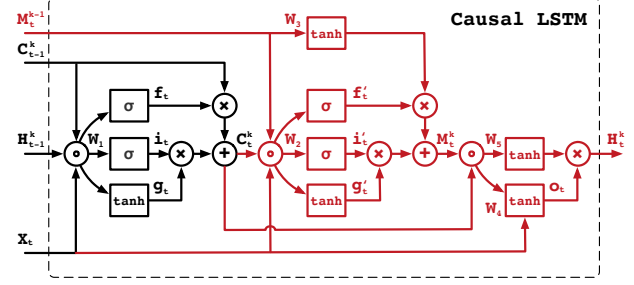


Figure 2. Causal LSTM, in which the temporal and spatial memories are connected in a cascaded way through gated structures. Colored parts are newly designed operations, concentric circles denote concatenation, and σ is the element-wise Sigmoid function.

memory directly depends on its previous state, \mathcal{C}_{t-1}^k , and is controlled through a forget gate, f_t , an input gate, i_t , and an input modulation gate, g_t . The current spatial memory, \mathcal{M}_t^k , depends on \mathcal{M}_{t-1}^{k-1} in the deep transition path. Specifically for the bottom layer ($k = 1$), we assign the topmost spatial memory at $t - 1$ to \mathcal{M}_t^{k-1} . Evidently different from the original spatiotemporal LSTM (Wang et al., 2017), causal LSTM adopts a cascaded mechanism, where the spatial memory is particularly a function of the temporal memory via another set of gate structures. Update equations in the k^{th} stacked causal LSTM can be presented as follows:

$$\begin{aligned}
 \begin{pmatrix} g_t \\ i_t \\ f_t \end{pmatrix} &= \begin{pmatrix} \tanh \\ \sigma \\ \sigma \end{pmatrix} W_1 * \begin{pmatrix} \mathcal{X}_t \\ \mathcal{H}_{t-1}^k \\ \mathcal{C}_{t-1}^k \end{pmatrix} \\
 \mathcal{C}_t^k &= f_t \odot \mathcal{C}_{t-1}^k + i_t \odot g_t \\
 \begin{pmatrix} g'_t \\ i'_t \\ f'_t \end{pmatrix} &= \begin{pmatrix} \tanh \\ \sigma \\ \sigma \end{pmatrix} W_2 * \begin{pmatrix} \mathcal{X}_t \\ \mathcal{C}_t^k \\ \mathcal{M}_{t-1}^{k-1} \end{pmatrix} \\
 \mathcal{M}_t^k &= f'_t \odot \tanh(W_3 * \mathcal{M}_{t-1}^{k-1}) + i'_t \odot g'_t \\
 o_t &= \tanh(W_4 * (\mathcal{X}_t, \mathcal{C}_t^k, \mathcal{M}_t^k)^T) \\
 \mathcal{H}_t^k &= o_t \odot \tanh(W_5 * (\mathcal{C}_t^k, \mathcal{M}_t^k)^T),
 \end{aligned} \tag{1}$$

where $*$ denotes the convolution operator, $W_{1 \sim 5}$ are the convolution weights, and σ is the element-wise Sigmoid function. The final output, \mathcal{H}_t^k , is co-determined by the dual memory states, \mathcal{M}_t^k and \mathcal{C}_{t-1}^k , as well as an output gate, o_t .

Evidently, this newly designed cascaded mechanism of the spatiotemporal memory states is superior to the simple concatenation, due to a significant increase in the recurrence depth along the deep transition pathway. It thus endows the predictive model with greater modeling capability for short-

term video dynamics and fine-grained spatial correlations.

We also consider another spatial-to-temporal causal LSTM variant. We swap the positions of the two memories, updating \mathcal{M}_t^k in the first place, and then calculating \mathcal{C}_t^k based on \mathcal{M}_t^k . An experimental comparison of these two alternative structures would be presented in Section 5, in which we would demonstrate that both of them lead to better video prediction results than the original spatiotemporal LSTM.

4.2. Gradient Highway Architecture

It is worth noting, although causal LSTMs alter the information flow in the deep transition paths, they follow the same way as the traditional stacked RNNs and the original PredRNN model in updating temporal memory states. Thus, merely organizing them in the PredRNN style, without any further improvement from the perspective of architecture, would hardly avoid gradient back-propagation difficulties.

For this purpose, we propose a recurrent architecture named *Gradient Highway*. It re-organizes causal LSTMs, keeping the gradients of the objective function with respect to certain hidden states from quickly vanishing during back-propagation. A schematic of this architecture is presented in Figure 3. We stack L causal LSTMs with temporal and deep transition connections, and particularly inject a gradient highway unit, as illustrated in the bottom subplot in Figure 3, between the 1st and the 2nd causal LSTM layers.

Intuitively, the gradient highway layer is necessary. Theoretical evidence indicates that highway layers (Srivastava et al., 2015b) enable easy training of very deep feed-forward networks. The gradient highway unit exploits this idea to the predictive recurrent model. Even though the temporal connections could deliver information horizontally in an efficient way, the long short-term memories along these temporal routes tend to “forget” the out-of-date information when it has almost no contributions to the present moment. In some situations, like temporary objects occlusions in videos, such a forgetting mechanism is not what we want. Instead, we need a direct route to deliver older but more correlated cues from the distant past. By using quickly updated hidden states, \mathcal{Z}_t , the gradient highway layer shows an alternative path, originating from the very first state, passing through the entire sequence, and reaching the final time step. While causal LSTMs learn short-term dynamics via complex deep transitions, the gradient highway layer still captures long-term correlations among distant video frames.

Note that the output activation of the bottom causal LSTM, \mathcal{H}_t^1 , is a function of, including but not limited to, the current input frame, \mathcal{X}_t , and the previous deep transition memory, \mathcal{M}_{t-1}^L . Residing above this layer, the gradient highway unit serves like a switch: it blocks out the deep transition paths of the hidden states, controlling the proportion of

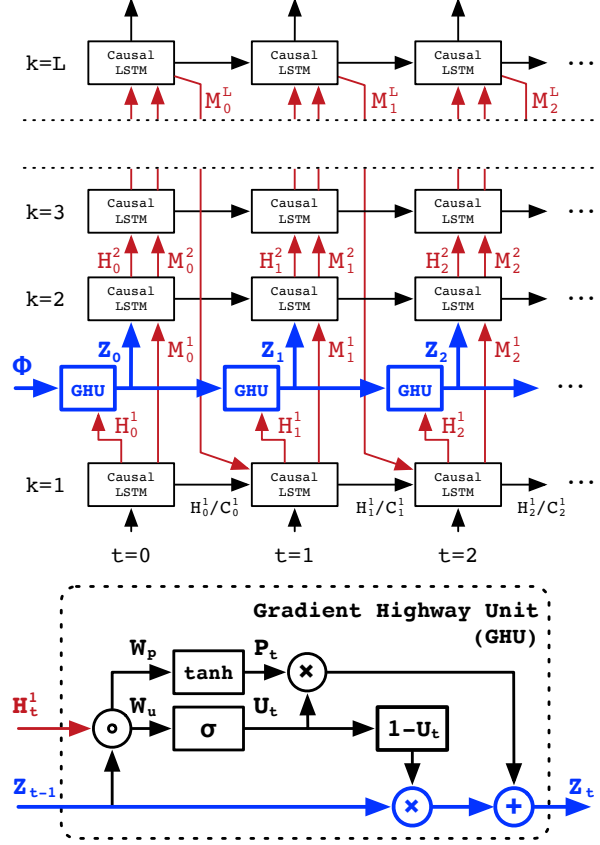


Figure 3. Final architecture (top) with the gradient highway unit (bottom), where concentric circles denote concatenation, and σ is the element-wise Sigmoid function. Blue parts indicate the gradient highway connecting the current time step directly with prior inputs, while the red parts show the deep transition pathway.

\mathcal{Z}_{t-1} and \mathcal{H}_t^1 through gated structures, \mathcal{P}_t and \mathcal{U}_t . The final PredRNN++ model organizes the above recurrent structures as a whole. Through the the gradient highway layer, it learns to weigh which one of the short-term or the long-term hidden representation is more correlated with future prediction targets. In this way, it absorbs knowledge from different time-scales in an adaptive mode. Key equations of the entire PredRNN++ model can be presented as follows:

$$\begin{aligned}
 \mathcal{H}_t^1, \mathcal{C}_t^1, \mathcal{M}_t^1 &= \text{CausalLSTM}_1(\mathcal{X}_t, \mathcal{H}_{t-1}^1, \mathcal{C}_{t-1}^1, \mathcal{M}_{t-1}^L) \\
 \mathcal{P}_t &= \tanh(W_{ph} * \mathcal{H}_t^1 + W_{pz} * \mathcal{Z}_{t-1}) \\
 \mathcal{U}_t &= \sigma(W_{uh} * \mathcal{H}_t^1 + W_{uz} * \mathcal{Z}_{t-1}) \\
 \mathcal{Z}_t &= \mathcal{U}_t \odot \mathcal{P}_t + (1 - \mathcal{U}_t) \odot \mathcal{Z}_{t-1} \\
 \mathcal{H}_t^2, \mathcal{C}_t^2, \mathcal{M}_t^2 &= \text{CausalLSTM}_2(\mathcal{Z}_t, \mathcal{H}_{t-1}^2, \mathcal{C}_{t-1}^2, \mathcal{M}_t^1) \\
 \mathcal{H}_t^k, \mathcal{C}_t^k, \mathcal{M}_t^k &= \text{CausalLSTM}_k(\mathcal{H}_t^{k-1}, \mathcal{H}_{t-1}^k, \mathcal{C}_{t-1}^k, \mathcal{M}_t^{k-1}), \quad (2)
 \end{aligned}$$

where $3 \leq k \leq L$. As mentioned, $*$ denotes the convolu-

tion operator, \odot denotes element-wise multiplication, $W_{\bullet\bullet}$ are the convolution weights, and σ is the element-wise Sigmoid function. Please refer to Equation (1) for detailed calculations inside each CausalLSTM unit.

We also explore other architecture variants by injecting the gradient highway unit into a different hidden layer slot, for example, between the $(L - 1)^{\text{th}}$ and L^{th} causal LSTMs. Experimental comparisons would be given in Section 5. The network discussed above outperforms the others, indicating the importance of modeling characteristics of raw inputs rather than the abstracted representations at higher layers.

As for network details, we observe that the numbers of the hidden state channels, especially those in lower layers, have strong impacts on the final prediction performance. We thus propose a 5-layer architecture, in pursuit of high prediction accuracy with reasonable training time and memory usage, consisting of 4 causal LSTMs with 128, 64, 64, 64 channels respectively, as well as an 128-channel gradient highway unit on the top of the bottom causal LSTM layer. We also set the convolution kernel size to 5 inside all recurrent units.

5. Experiments

To measure the performance of PredRNN++, we use two video prediction datasets: a synthetic dataset with moving digits and a real video dataset with human actions. The results prove the superior performance of our approach. We train all compared models using TensorFlow (Abadi et al., 2016) and optimize them to convergence using ADAM (Kingma & Ba, 2015) with a starting learning rate of 10^{-3} . Besides, we apply the scheduled sampling strategy (Bengio et al., 2015) to all of the models to stitch the discrepancy between training and inference. As for the objective function, we combine the traditional $L1$ and $L2$ loss to simultaneously enhance the sharpness of the foreground objects and guarantee the smoothness of the general image appearance.

5.1. Moving MNIST Dataset

Implementation We follow the experimental setups in (Srivastava et al., 2015a; Wang et al., 2017) on the Moving MNIST dataset, predicting 10 future frames given 10 previous inputs. Each frame contains 2 handwritten digits bouncing inside a 64×64 grid of image. Before feeding input sequence to the network, we convert pixel values into the range $[0, 1]$. To assure the trained model has never seen the digits during inference period, we sample digits from different parts of the original MNIST dataset to construct our training set and test set. The dataset volume is fixed, with 10,000 sequences for the training set, 3,000 sequences for the validation set and 5,000 sequences for the test set. During training, the mini-batch size is set to 8 and the training process is stopped after 100,000 iterations. To measure the

generalization and transfer ability, we evaluate all models trained with 2 moving digits on another 3 digits test set.

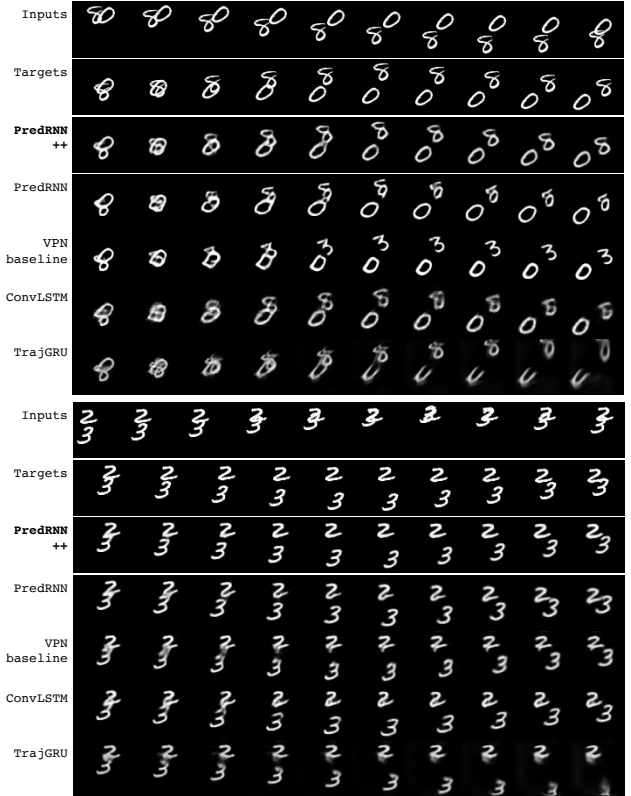


Figure 4. Two prediction examples respectively with entangled digits in the input or output frames on Moving MNIST-2 test set.

Results To evaluate the performance of our model, we measure the per-frame structural similarity index measure (SSIM) (Wang et al., 2004), the mean square error (MSE) and the mean absolute error (MAE). Table 1 illustrates these metrics compared with prior methods. We include the Video Pixel Networks (VPN) (Kalchbrenner et al., 2017) as a strong competitor, using its baseline version that generates each frame in one pass. Our models fully outperform the VPN baseline as well as other methods in all three metrics.

Figure 5 illustrates the frame-wise MSE results by all of the compared models. Our approach achieves the best result at every time step. For all models, the prediction quality degrades over time. But compared with VPN and PredRNN, our approach yields a less degradation rate, indicating a more powerful capability to capture long-term dependencies. Additionally, such inevitable degradations reveal the inherent uncertainty of future. Modeling this uncertainty by variational auto-encoders or adversarial networks is an interesting direction. Serving as a training paradigm, adversarial networks can be easily applied to our model. In this paper, we would like to concentrate on the network architecture,

Table 1. Results of PredRNN++ comparing with other models. We report per-frame SSIM, MSE and MAE of generated sequences. Higher SSIM or lower MSE/MAE denotes higher accuracy. (*) indicates models that are not open source and are reproduced by us or others.

MODEL	MNIST-2			MNIST-3		
	SSIM	MSE	MAE	SSIM	MSE	MAE
FC-LSTM (SRIVASTAVA ET AL., 2015A)	0.690	118.3	209.4	0.651	162.4	310.6
CONVLSTM (SHI ET AL., 2015)	0.707	103.3	182.9	0.673	142.1	281.5
TRAJGRU (SHI ET AL., 2017)	0.713	106.9	190.1	0.682	134.0	259.7
CDNA (FINN ET AL., 2016)	0.721	97.4	175.3	0.669	138.2	256.1
DFN (DE BRABANDERE ET AL., 2016)	0.726	89.0	172.8	0.679	140.5	272.6
VPN* (KALCHBRENNER ET AL., 2017)	0.870	64.1	131.0	0.734	112.3	247.5
PREDRNN (WANG ET AL., 2017)	0.867	56.8	126.1	0.782	93.4	214.9
CAUSAL LSTMS + PREDRNN ARCHITECTURE	0.882	52.5	114.6	0.795	89.2	203.5
CAUSAL LSTMS (SPATIAL TO TEMPORAL VARIANT)	0.875	54.0	120.1	0.784	91.8	210.4
GRADIENT HIGHWAY + ST-LSTMS	0.886	50.7	115.3	0.790	88.9	207.6
GRADIENT HIGHWAY + CAUSAL LSTMS (PREDRNN++)	0.898	46.5	106.8	0.814	81.7	190.8

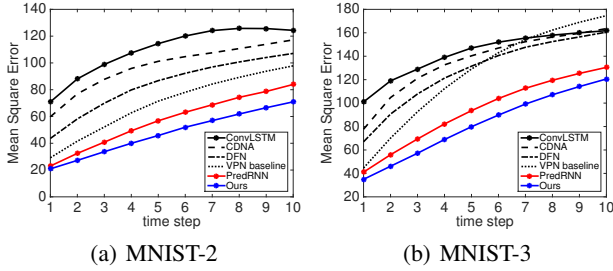


Figure 5. Frame-wise MSE over the test sets, produced by different models trained on MNIST-2. Lower curves denote higher accuracy.

leaving the exploration of these techniques as future work. In Figure 4, we show comparisons of the predicted frames by all of the compared models. With causal memories, our model makes the most accurate predictions of digit trajectories. We also observe that the most challenging task in future predictions is to maintain the shape of the digits after occlusion happens. This scenario requires our model to learn from previously distant contexts. For example, in the first case in Figure 4, two digits entangle with each other at the beginning of the target future sequence. Most prior models fail to preserve the correct shape of digit “8”, since their outcomes mostly depend on high level representations at nearby time steps, rather than the distant previous inputs (please see our afterwards gradient analysis). Similar situations happen in the second sample, all compared models present various but incorrect shapes of digit “2” in predicted frames, while PredRNN++ maintains its appearance. It is the gradient highway architecture that enables our approach to learn more disentangled representations and predict both correct shapes and trajectories of moving objects.

Ablation Study As shown in Table 1, replacing the spatiotemporal LSTMs (ST-LSTMs) with causal LSTMs improves the performance of PredRNN (SSIM from 0.867 up

Table 2. Ablation study: a comparison among the variants of the gradient highway architecture. Models differentiate with each other in the location of the gradient highway unit.

MODEL	SSIM	MSE
GRADIENT HIGHWAY (TOP)	0.885	52.0
GRADIENT HIGHWAY (MIDDLE)	0.894	48.1
FINAL: GRADIENT HIGHWAY (BOTTOM)	0.898	46.5

to 0.882). This result demonstrates the superiority of the cascaded structure (causal LSTM) over the simple concatenation (ST-LSTM) in increasing the recurrence depth. We then explore a variant structure of causal LSTM, where the positions of spatial and temporal memories are swapped. This structure (0.875) also outperforms ST-LSTMs (0.867), but underperforms our proposed version of causal LSTM (0.882). Note that the gradient highway architecture further boosts all of these performance.

In Table 2, we compare the gradient highway architecture with its variants, which inject the gradient highway unit into other hidden layer slots. All compared models use the same causal LSTMs. Our proposed network that resides the gradient highway unit right above the bottom causal LSTM performs the best, indicating the importance to switch the data flow between the input frames, the long-term highway states, and the memories along the deep transition pathways.

Gradient Analysis Figure 7 evaluates the ability of all compared deep-in-time architectures to capture long-term dependencies by overcoming the vanishing gradient issue. We observe that the moving digits are frequently entangled, indicating object occlusions in the real world. It is difficult to maintain the shapes of the entangled digits, since deep-in-time networks tend to rely on short-term video appearance but “forget” prior input frames. We count the frequency of

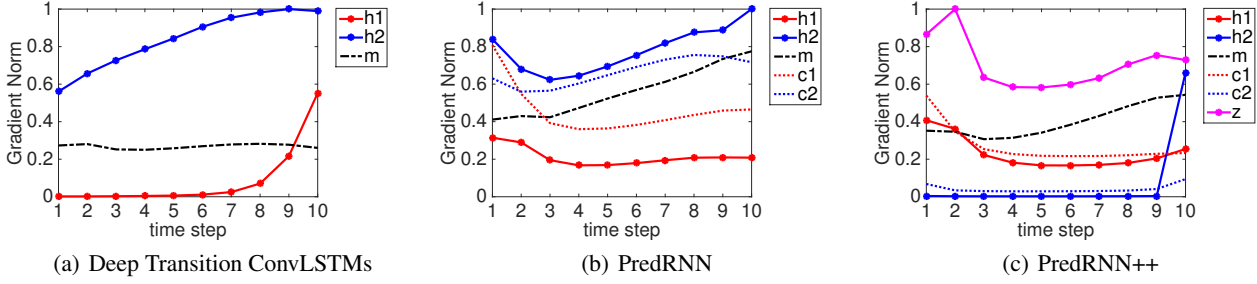


Figure 6. The gradient norm of the loss function at the last time step, \mathcal{L}_{20} , with respect to intermediate activities in the encoder, including hidden states, temporal memory states and the spatial memory states averaged by layers: $\|\nabla_{\mathcal{H}_t^k} \mathcal{L}_{20}\|$, $\|\nabla_{\mathcal{C}_t^k} \mathcal{L}_{20}\|$, and $\|\nabla_{\mathcal{M}_t} \mathcal{L}_{20}\|$.

digit entangling in each of the 10 input frames across the whole test set. As shown in Figure 7(a), more occlusions occur from the 4th to the 9th time step. Correspondingly, Figure 7(b) illustrates the gradient norm of the loss function at the last time step with respect to each input frame: $\|\nabla_{\mathcal{X}_t} \mathcal{L}_{20}\|$ where $1 \leq t \leq 10$. Note that all compared recurrent models, but our proposed PredRNN++ with gradient highway architecture, suffer from the vanishing gradient problem, where the derivatives steeply decay as we trace back in time. Considering the challenging ‘‘occlusion’’ scenarios, the gradient highway connections endow our model with the capability to learn from the most correlated contexts. The trend of this gradient curve shows that PredRNN++ manages to ease vanishing gradients and model long-term dependencies by providing gradient flows with shorter paths from later outputs to distant previous inputs.

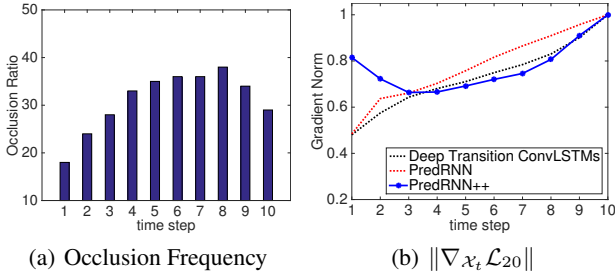


Figure 7. Gradient analysis: (a) The frequency of digits entangling in each input frame among 5,000 sequences over the test set. (b) The gradient norm of the loss function at the last time step with respect to each input frame, averaged over the whole test set.

Figure 6 analyzes by what means our approach eases the vanishing gradient problem, illustrating the absolute values of the loss function derivatives at the last time step with respect to intermediate hidden states and memory states: $\|\nabla_{\mathcal{H}_t^k} \mathcal{L}_{20}\|$, $\|\nabla_{\mathcal{C}_t^k} \mathcal{L}_{20}\|$, and $\|\nabla_{\mathcal{M}_t} \mathcal{L}_{20}\|$. The vanishing gradient problem leads the gradients to decrease from the top layer down to the bottom layer. For simplicity, we ana-

lyze recurrent models consisting of 2 layers. In Figure 6(a), the gradient of \mathcal{H}_t^1 vanishes rapidly back in time, indicating that previous true frames yield negligible influence on the last frame prediction. With temporal memory connections \mathcal{C}_t^1 , the PredRNN model in Figure 6(b) provides the gradient a shorter pathway from previous bottom states to the top. As the curve of \mathcal{H}_t^1 arises back in time, it emphasizes the representations of the more correlated hidden states. In Figure 6(c), the gradient highway states \mathcal{Z}_t hold the largest derivatives while $\|\nabla_{\mathcal{H}_t^2} \mathcal{L}_{20}\|$ decays steeply back in time, indicating that gradient highway stores long-term dependencies and allows causal LSTMs to concentrate on capturing short-term spatiotemporal dynamics. By explicitly disentangling short-term and long-term dynamics, PredRNN++ yields more explainable results and performs more robust against complex variations.

5.2. KTH Action Dataset

The KTH action dataset (Schuldt et al., 2004) contains 6 types of human actions (walking, jogging, running, boxing, hand waving and hand clapping) in different scenarios: indoors and outdoors with scale variations or different clothes. Each video clip has a length of four seconds in average and was taken with a static camera in 25 fps frame rate.

Implementation We adopt the experiment setup in (Villegas et al., 2017a; Wang et al., 2017), dividing videos clips across all 6 action categories into a training set of 108,717 sequences (persons 1-16) and a test set of 4,086 sequences (persons 17-25), and resizing all video frames into shapes of 128×128 pixels. We train all of the compared models by making them generate the subsequent 10 frames from prior 10 frames, with the combined $L1 + L2$ objective function across all time steps including both the encoder and decoder stages. The mini-batch size is 4 and the training process is stopped after 200,000 iterations. At inference, we extend the prediction horizon to 20 future time steps.

Results At first, we notice an important property of this dataset: **the periodic patterns in human actions**. Though few occlusions exist due to monotonous actions and plain backgrounds, predicting a longer video sequence accurately is still difficult in preliminaries works, probably resulting from the inherent vanishing gradient problem of deep-in-time networks. The key to this problem is to capture distant cues, here, indicating human behaviors happening repeatedly, such as the alternating movements of a person’s arms and legs when she/he is walking. The prediction results on this dataset measure the ability of our approach to model the periodic spatiotemporal data, as shown in Figure 9.

Table 3. A quantitative evaluation of different methods on the KTH human action test set. These metrics are averaged over the 20 predicted frames. A higher score denotes a better prediction accuracy.

MODEL	PSNR	SSIM
CONVLSTM (SHI ET AL., 2015)	23.58	0.712
TRAJGRU (SHI ET AL., 2017)	26.97	0.790
DFN (DE BRABANDERE ET AL., 2016)	27.26	0.794
MCNET (VILLEGAS ET AL., 2017A)	25.95	0.804
PREDRNN (WANG ET AL., 2017)	27.55	0.839
PREDRNN++	28.47	0.865

In Table 3 and Figure 8, we further assess the prediction results on the human action dataset using image-level PSNR and SSIM. Our approach consistently outperforms prior methods. In particular, we adopt the results of MCnet and ConvLSTMs reported in (Villegas et al., 2017a), since we follow the same experimental setups. The performance of these models degrades quickly over time, since they are trained for 10 future time steps but tested for up to 20 time steps. To make the results comparable, we apply identical settings to our model. By contrast, gradual declines in metric curves are observed for the last 10 time steps. Compared with the latest state-of-the-art, our approach performs better in every future time step, indicating a great power to capture both short-term and long-term spatiotemporal dynamics.

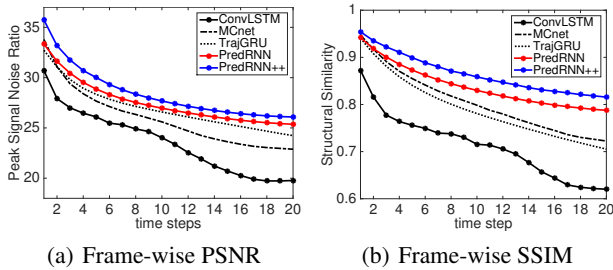


Figure 8. Frame-wise PSNR and SSIM comparisons of different models on the KTH test set. Higher curves denote better results.

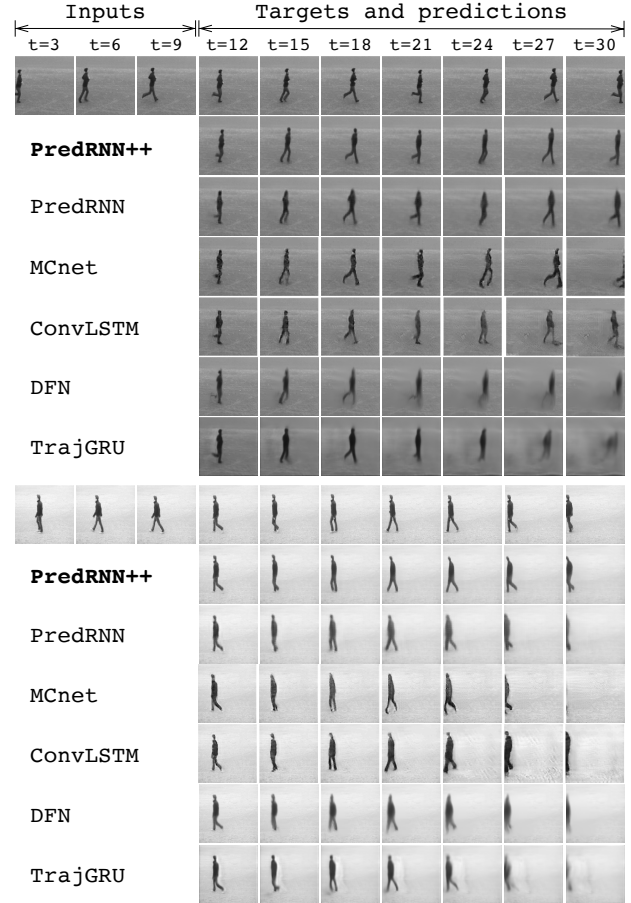


Figure 9. KTH prediction samples. We predict 20 frames into the future by observing 10 frames. Frames are shown at a three frames interval. Note that these sequences were also used for presentations in prior works (Villegas et al., 2017a; Wang et al., 2017).

6. Conclusions

In this paper, we presented a predictive recurrent network named PredRNN++, towards a resolution of the spatiotemporal predictive learning dilemma between deep-in-time structures and vanishing gradients. To maximize the modeling capability of our approach to short-term variations, we designed an improved dual memory recurrent structure, Causal LSTM, connecting the spatial and temporal memory states in a cascaded mechanism. To ease the vanishing gradient problem, we proposed a gradient highway architecture, which provided gradients shorter paths from future predictions back to distant previous inputs. By evaluating PredRNN++ on a synthetic moving digits dataset with severe object occlusions, and a real video dataset with periodic human actions, we demonstrated that it is able to obtain explainable and state-of-the-art prediction results by learning both long-term and short-term dependencies adaptively.

References

- Abadi, Martín, Agarwal, Ashish, Barham, Paul, Brevdo, Eugene, Chen, Zhifeng, Citro, Craig, Corrado, Greg S, Davis, Andy, Dean, Jeffrey, Devin, Matthieu, et al. Tensorflow: Large-scale machine learning on heterogeneous distributed systems. *arXiv preprint arXiv:1603.04467*, 2016.
- Bengio, Samy, Vinyals, Oriol, Jaitly, Navdeep, and Shazeer, Noam. Scheduled sampling for sequence prediction with recurrent neural networks. In *Advances in Neural Information Processing Systems*, pp. 1171–1179, 2015.
- Bengio, Yoshua, Simard, Patrice, and Frasconi, Paolo. Learning long-term dependencies with gradient descent is difficult. *IEEE transactions on neural networks*, 5(2): 157–166, 1994.
- Bhattacharjee, Prateep and Das, Sukhendu. Temporal coherency based criteria for predicting video frames using deep multi-stage generative adversarial networks. In *Advances in Neural Information Processing Systems*, pp. 4271–4280, 2017.
- Bianchini, Monica and Scarselli, Franco. On the complexity of neural network classifiers: A comparison between shallow and deep architectures. *IEEE transactions on neural networks and learning systems*, 25(8):1553–1565, 2014.
- De Brabandere, Bert, Jia, Xu, Tuytelaars, Tinne, and Van Gool, Luc. Dynamic filter networks. In *NIPS*, 2016.
- Denton, Emily L, Chintala, Soumith, Fergus, Rob, et al. Deep generative image models using a laplacian pyramid of adversarial networks. In *NIPS*, pp. 1486–1494, 2015.
- Finn, Chelsea, Goodfellow, Ian, and Levine, Sergey. Unsupervised learning for physical interaction through video prediction. In *NIPS*, 2016.
- Goodfellow, Ian J., Pougetabadie, Jean, Mirza, Mehdi, Xu, Bing, Wardefarley, David, Ozair, Sherjil, Courville, Aaron, and Bengio, Yoshua. Generative adversarial networks. *NIPS*, 3:2672–2680, 2014.
- Hochreiter, Sepp and Schmidhuber, Jürgen. Long short-term memory. *Neural computation*, 9(8):1735–1780, 1997.
- Kalchbrenner, Nal, Oord, Aaron van den, Simonyan, Karen, Danihelka, Ivo, Vinyals, Oriol, Graves, Alex, and Kavukcuoglu, Koray. Video pixel networks. In *ICML*, 2017.
- Kingma, Diederik and Ba, Jimmy. Adam: A method for stochastic optimization. In *ICLR*, 2015.
- Lerer, Adam, Gross, Sam, and Fergus, Rob. Learning physical intuition of block towers by example. In *ICML*, 2016.
- Lotter, William, Kreiman, Gabriel, and Cox, David. Deep predictive coding networks for video prediction and unsupervised learning. In *International Conference on Learning Representations (ICLR)*, 2017.
- Lu, Chaochao, Hirsch, Michael, and Schölkopf, Bernhard. Flexible spatio-temporal networks for video prediction. In *Proceedings of the IEEE Conference on Computer Vision and Pattern Recognition*, pp. 6523–6531, 2017.
- Mathieu, Michael, Couprie, Camille, and LeCun, Yann. Deep multi-scale video prediction beyond mean square error. In *ICLR*, 2016.
- Oh, Junhyuk, Guo, Xiaoxiao, Lee, Honglak, Lewis, Richard L, and Singh, Satinder. Action-conditional video prediction using deep networks in atari games. In *NIPS*, pp. 2863–2871, 2015.
- Pascanu, Razvan, Mikolov, Tomas, and Bengio, Yoshua. On the difficulty of training recurrent neural networks. *ICML*, 28:1310–1318, 2013.
- Patraucean, Viorica, Handa, Ankur, and Cipolla, Roberto. Spatio-temporal video autoencoder with differentiable memory. In *ICLR Workshop*, 2016.
- Ranzato, MarcAurelio, Szlam, Arthur, Bruna, Joan, Mathieu, Michael, Collobert, Ronan, and Chopra, Sumit. Video (language) modeling: a baseline for generative models of natural videos. *arXiv preprint arXiv:1412.6604*, 2014.
- Rumelhart, David E, Hinton, Geoffrey E, and Williams, Ronald J. Learning representations by back-propagating errors. *Cognitive modeling*, 5(3):1, 1988.
- Schuldt, Christian, Laptev, Ivan, and Caputo, Barbara. Recognizing human actions: a local svm approach. In *International Conference on Pattern Recognition*, pp. 32–36 Vol.3, 2004.
- Shi, Xingjian, Chen, Zhourong, Wang, Hao, Yeung, Dit-Yan, Wong, Wai-Kin, and Woo, Wang-chun. Convolutional lstm network: A machine learning approach for precipitation nowcasting. In *NIPS*, pp. 802–810, 2015.
- Shi, Xingjian, Gao, Zhihan, Lausen, Leonard, Wang, Hao, Yeung, Dit-Yan, Wong, Wai-kin, and Woo, Wang-chun. Deep learning for precipitation nowcasting: A benchmark and a new model. In *Advances in Neural Information Processing Systems*, 2017.
- Srivastava, Nitish, Mansimov, Elman, and Salakhutdinov, Ruslan. Unsupervised learning of video representations using lstms. In *ICML*, 2015a.

- Srivastava, Rupesh K, Greff, Klaus, and Schmidhuber, Jürgen. Training very deep networks. In *Advances in neural information processing systems*, pp. 2377–2385, 2015b.
- van den Oord, Aaron, Kalchbrenner, Nal, Espeholt, Lasse, Vinyals, Oriol, Graves, Alex, et al. Conditional image generation with pixelcnn decoders. In *NIPS*, pp. 4790–4798, 2016.
- Villegas, Ruben, Yang, Jimei, Hong, Seunghoon, Lin, Xunyu, and Lee, Honglak. Decomposing motion and content for natural video sequence prediction. In *International Conference on Learning Representations (ICLR)*, 2017a.
- Villegas, Ruben, Yang, Jimei, Zou, Yuliang, Sohn, Sungryull, Lin, Xunyu, and Lee, Honglak. Learning to generate long-term future via hierarchical prediction. *arXiv preprint arXiv:1704.05831*, 2017b.
- Vondrick, Carl, Pirsaviash, Hamed, and Torralba, Antonio. Generating videos with scene dynamics. In *Advances In Neural Information Processing Systems*, pp. 613–621, 2016.
- Wang, Yunbo, Long, Mingsheng, Wang, Jianmin, Gao, Zhifeng, and Philip, S Yu. Predrnn: Recurrent neural networks for predictive learning using spatiotemporal lstms. In *Advances in Neural Information Processing Systems*, pp. 879–888, 2017.
- Wang, Zhou, Bovik, A. C, Sheikh, H. R, and Simoncelli, E. P. Image quality assessment: from error visibility to structural similarity. *TIP*, 13(4):600, 2004.
- Werbos, Paul J. Backpropagation through time: what it does and how to do it. *Proceedings of the IEEE*, 78(10): 1550–1560, 1990.
- Williams, Ronald J and Zipser, David. Gradient-based learning algorithms for recurrent networks and their computational complexity. *Backpropagation: Theory, architectures, and applications*, 1:433–486, 1995.
- Zhang, Junbo, Zheng, Yu, and Qi, Dekang. Deep spatiotemporal residual networks for citywide crowd flows prediction. In *AAAI*, pp. 1655–1661, 2017.
- Zilly, Julian Georg, Srivastava, Rupesh Kumar, Koutník, Jan, and Schmidhuber, Jürgen. Recurrent highway networks. In *ICML*, 2017.